energies

MDPI

Article

The Effect of Single Sandstone Stacking Pattern on the Sandstone Reservoir Physical Properties—A Case Study from the Shanxi Formation in the Daniudi Area, Northeastern Ordos Basin

Yun He [1], Hengwei Guo [2], Haoxiang Lan [2], Can Ling [2] and Meiyan Fu [2,3,*]

[1] Sinopec, North China Oil and Gas Field Exploration and Development Research Institute, Zhengzhou 450006, China; heyun.hbsj@sinopec.com
[2] College of Energy, Chengdu University of Technology, Chengdu 610059, China; lg0111@stu.cdut.edu.cn (H.G.); lanhaoxiang@stu.cdut.edu.cn (H.L.); lingcan@stu.cdut.edu.cn (C.L.)
[3] State Key Laboratory of Oil and Gas Reservoir Geology and Exploitation, Chengdu University of Technology, Chengdu 610059, China
* Correspondence: fumeiyan08@cdut.cn; Tel.: +86-185-0283-0103

Abstract: The role of the single sandstone stacking pattern in controlling the physical properties of the sandstones deposited in the distribution channels of the deltaic plain is unclear. This study aims to reveal the effect of the single sandstone packing patterns on the reservoir qualities of sandstones from the Shanxi Formation in the Daniudi gas field of Ordos Basin. Based on the core observation, 2D-image analysis, and thin section identification, the lithofacies were identified, the stacking patterns of the single sandbody were divided, and the differences in minerals composition and diagenesis of different sandstone stacking patterns were analyzed. According to the sedimentary facies analysis, 10 types of lithofacies have been identified in the Shanxi Formation in the study area. The single sandstone stacking patterns include mixed stacking patterns of coarse to medium-grained sandstone, fining upwards stacking patterns of coarse- to medium-grained sandstone, and coarsening upwards stacking patterns of fine- to coarse-grained sandstone. Among these single sandstone stacking patterns, there is a greater percentage of lithofacies with high reservoir quality in the fining upwards stacking patterns of coarse- to medium-grained sandstone. Through a comparative study of the differences in minerals composition, the degree of compaction, and dissolution of sandstones, it is suggested that the high porosities and permeabilities of the coarse- to medium-grained sandstone lithofacies in the fining upwards stacking patterns are caused by the low content of the matrix in sandstone, relatively weak compaction, relatively high amounts of primary pores, and strong dissolution. The relatively high content of rigid clastic particles with coarser-grained size was favorable for the preservation of primary pores. The relatively high primary porosity could provide favorable passages for the late diagenetic fluid, leading to the development of dissolved pores. The study can provide an important basis for the exploration of high-quality sandstone reservoirs in the distributary channels of the delta plain.

Keywords: Ordos Basin; Shanxi Formation; lithofacies; sandstone stacking pattern; compaction; dissolution

Citation: He, Y.; Guo, H.; Lan, H.; Ling, C.; Fu, M. The Effect of Single Sandstone Stacking Pattern on the Sandstone Reservoir Physical Properties—A Case Study from the Shanxi Formation in the Daniudi Area, Northeastern Ordos Basin. *Energies* **2022**, *15*, 4740. https://doi.org/10.3390/en15134740

Academic Editors: Mofazzal Hossain and Reza Rezaee

Received: 11 May 2022
Accepted: 27 June 2022
Published: 28 June 2022

1. Introduction

The exploration of sandstone with high reservoir quality deposited in the delta distributary channel is the main research object of conventional oil and gas exploration and development [1]. The development of high-quality sandstones is generally controlled by sedimentation, with a minor influence of diagenesis. The sedimentation could induce a change in grain size, bedding type, and mineral composition. As the product of sedimentation, lithofacies are used to evaluate the quality of a sandstone reservoir. It is widely recognized that the physical properties of sandstone reservoirs are generally correlative

with lithofacies types [2–4]. However, in the different lithofacies assembly, the porosity and permeability of the same lithofacies could be different. The assembly of lithofacies is related to the change in sedimentary hydrodynamic conditions and the architecture of the sandbody. As a result, there will be a different single sandstone stacking pattern.

The analysis of the single sandstone stacking pattern was rarely used to evaluate the reservoir quality of sandstones [5]. The single sandstone stacking pattern refers to the vertical variation of the sedimentary structure, including lithology, mineral composition, texture, color, and so on. According to the variation of particle size, there are two sedimentary sequences in the sedimentology, a fining-upwards sequence and a coarsening-upwards sequence [6]. Du (2013) [6] suggest that sandstone stacking patterns can be divided into a coarsening-upwards stacking pattern, fining-upwards stacking pattern, and mixed stacking pattern, according to the variation of grain size. Sandstone stacking pattern analysis can reflect the characteristic of sedimentary hydrodynamic conditions. Kathleen et al. (2010) [7] reported that the change in grain sizes, grain sorting, and matrix contents could result from the change of energy in the sedimentary environment. The coarsening upward stacking pattern represents an increase in the energy of the sedimentary environment. The fining-upwards stacking pattern is the reverse. The different sandstone stacking patterns usually have a different composition of sedimentary material. The provenance of sedimentation could be an important influencing factor for the change of composition of sedimentary material [8]. The lithofacies in the different sandstone stacking patterns could have different grain sorting, which has a great impact on the compaction [9]. In summary, there are many gaps in the research on the effect of different sandstone stacking patterns on the physical properties of sandstone.

As the potential factor controlling the quality of a sandstone reservoir, the single sandstone packing patterns could be identified using the logging well characteristic. Due to the different porosity and matrix contents in the different single sandstone packing patterns, there are distinguished logging responses. Based on the particular well logging curve, each sandstone packing pattern is easy to identify and predict. Therefore, the sandstone packing pattern can be used as an important unit to evaluate the quality of the sandstone reservoir.

The Lower Permian Shanxi Formation accounts for 70% of the unexploited reserves of the Daniudi gasfield in Ordos Basin, with a good prospect for natural gas development. Previous studies have been conducted on the porosity and permeability of lithofacies from the Shanxi Formation [10,11]. Due to the division of a single sandstone stacking pattern, the influencing factor for the porosity and permeability of sandstone reservoirs is not clear; the reservoir prediction in the Shanxi Formation is constrained in the present. The Lower Permian Shanxi Formation in the study area was deposited in the distributary channel of the delta plain, dominated by medium- to coarse-grained litharenite and quartz arenite [10,11]. The dissolution could be observed in the sandstone from the Shanxi Formation, which has some influence on the physical properties [6]. This study aims to reveal the effect of a single sandstone stacking pattern on the physical properties of a sandstone reservoir. Based on the core description, the lithofacies and single sandstone stacking patterns were divided. Through the core observation and X-ray diffraction analysis, the lithological characteristic of the Shanxi Formation was analyzed. The types of diagenetic alteration were analyzed using thin sections and cathode luminescence observations. The types of pores were determined, and quantitative statistics of pore types were performed by thin section two-dimensional image analysis. The comparative study of lithology, grain size, matrix content, the degree of compaction, and dissolution of different lithofacies and single sandstone stacking patterns was performed to discuss the control of single sandstone stacking patterns on the physical properties of sandstone reservoirs.

2. Geological Setting

The Daniudi gas field is located in the border area between Yulin City, Shanxi Province, and Yjinholuo Banner and Wuzheng Banner, Inner Mongolia Autonomous Region in China, covering an area of 2000 km^2. Tectonically, the field is located in the northeastern part of the

Yishan slope of the Ordos Basin (Figure 1). The basin is adjacent to the Loop Basin in the north across the Ulangar Bedrock Bulge, with the south across the Weibei Flexural Belt and the Weihe Basin. The east is in the Jinxi Flexural Belt and the Luliang Uplift, and the west of the Liupan Mountains and the Yinchuan Basin via the Masking Tectonic Belt [12], which is generally a gentle monocline, high in the northeast and low in the southwest [13,14]. The tectonic structures and fractures are not developed in the study area, only with local nose-like uplifts, and no large tectonic traps have been formed [10,15]. Influenced by the humid paleoclimate, marshes occurred commonly during the deposition period of the Shanxi Formation [16], multiple sets of coal seams were developed. During the early deposition of the Shanxi Formation, the northern source area was rapidly uplifted due to tectonic activity [17–19], resulting in a large sandbody developing in the study area. In the Early Permian Shanxi period, sediment was deposited in the delta of the sea–land transition. The lower part of the Shanxi Formation developed in the delta front, and the upper part developed in the delta plain [20–23]. The deposition period of the Shanxi Formation is the period of terrestrial sedimentary facies development in the Ordos area. Due to the change of climatic conditions from humid to arid and the large imbalance of tectonic activities on the north and south margins, there was a retention of the remnant marine interlayer in the early deposition period of the Shanxi Formation, resulting in the development of the gray and gray-black sandstone in this period. Furthermore, a few marine sediments were retained in the southeast of the study area. The delta plain of the Shanxi Formation includes the subfacies of the distributary channel, distributary channel bay, natural levee, flood fan, floodplain, and swamp. The delta front includes the subfacies of the underwater distributary channel, underwater distributary channel bay, and mouth bar [24,25]. According to the sedimentary cycle, the Shanxi Formation was divided into the Shan 1 and Shan 2 members from the bottom to top and can be further subdivided into five sub-members from S1-1 to S2-2 (Figure 1). The lithology of the Shan 1 member is conglomeratic sandstone, conglomeratic coarse sandstone, coarse sandstone, medium sandstone, fine sandstone, and mudstone. The coal seam is frequently developed in the Shan 1 member. The lithology of the Shan 2 member is basically the same as that of the Shan 1 member, but the thickness of the coal seam is thinner than the Shan 1 member [26,27].

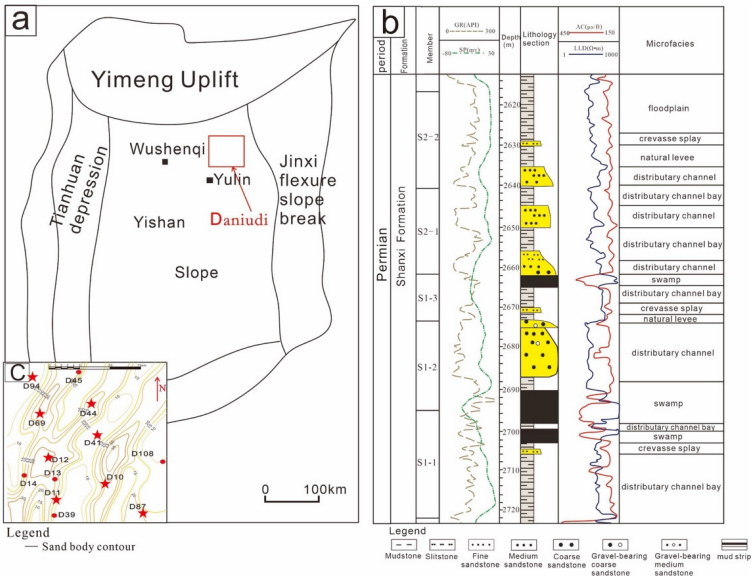

Figure 1. Location of the study area and stratigraphic column of the Shanxi Formation. (**a**) Tectonic zoning map. (**b**) Stratigraphic column of the well D10. (**c**) The contour map of sandstone thickness in the Daniudi Field (red star-the drilling cored well; red circle-the drilling well).

3. Materials and Methods

There are 72 samples of the Shanxi Formation collected from the 10 drilling cored wells in the Daniudi gas field. The cores were observed, and the sedimentary structures were identified. Seventy-two thin sections were observed and identified using a microscope (DM4500, Leica, Weztlar, Germany). Based on the thin section observations, the content of quartz, feldspar, and lithic fragments were counted point by point. The composition of minerals of sandstones from the Shanxi Formation was detected by XRD using A DMAX-3C X-ray diffractometer (Rigaku Corporation, Tokyo, Japan). The sandstone grain size was automatically analyzed by 2D image analysis software (Chuanda image analysis software, Chengdu, China). The samples were observed under SEM using a Quanta 250 FEG (FEI Company, Hillsboro, OR, USA) and an INCA x-max20 (Energy Disperse Spectroscopy, Oxford Instruments, Abingdon, UK). The porosities and permeabilities of sandstones were measured using the gas method. The relative deviation for porosity determinations was 0.5–1.5%, and that of permeability was $\leq$10% for low permeability samples.

4. Results

4.1. Petrographic Characteristic

There are different sedimentary structures in the sandstones from the Shanxi Formation deposited in the distributary channel, mainly including graded bedding, trough cross-bedding, plate cross-bedding, small cross-bedding, wedge cross-bedding, and parallel bedding. Bedding and grain size of sandstone could be used to reflect the sedimentary hydrodynamic condition [28–30]. According to the sedimentary structures and differences in grain size, the lithofacies can be mainly divided into ten types in the Shanxi Formation (Figure 2), as shown in Table 1.

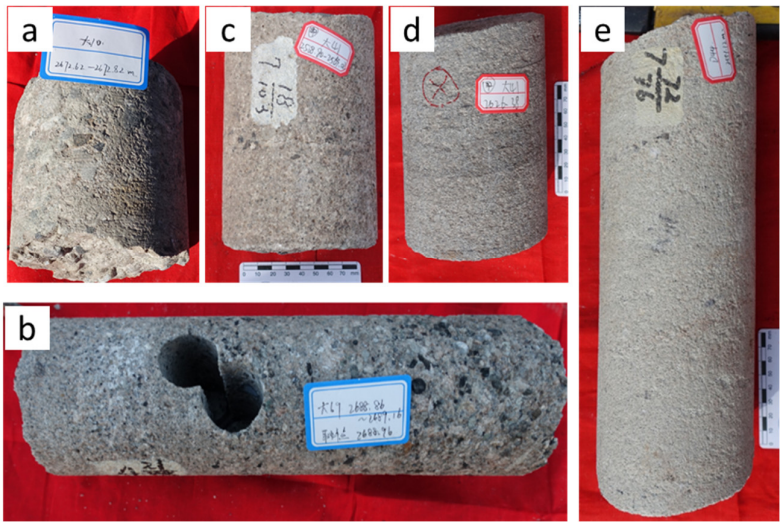

Figure 2. The sandstones with different grain sizes in the Shanxi Formation (from the description of cores). (**a**) Fine-grained conglomerate, well D10; (**b**) conglomeratic sandstone, well D67; (**c**) gravel-bearing coarse sandstone, well D41; (**d**) coarse sandstone, well D41; (**e**) medium sandstone, well D44.

Table 1. The lithofacies of the Shanxi Formation in the Daniudi area (from the description of cores).

Size Grading	Sedimentary Structures	Lithofacies
fine-grained conglomerate	massive	massive fine-grained conglomerate
conglomeratic sandstone	graded bedding	graded bedding conglomeratic sandstone
gravel-bearing coarse sandstone	massive	massive gravel-bearing coarse sandstone
coarse sandstone	plate cross-bedding massive	plate cross-bedding coarse sandstone massive coarse sandstone
medium-coarse sandstone	massive trough cross-bedding	massive medium-coarse sandstone trough cross-bedding medium-coarse sandstone
medium sandstone	massive parallel bedding small cross-bedding	massive medium sandstone parallel bedding medium sandstone small cross-bedding medium sandstone

Based on the thin section observations of 72 samples in the study area, the Shanxi Formation mainly develops quartz arenite and litharenite. Based on the thin section observation, the average contents of quartz, feldspar, and lithic fragments were 62.6%, 5.45%, and 35.85%, respectively. There was a medium compositional maturity of sandstones; the types of lithic fragments included mainly sedimentary lithic fragments and metamorphic and volcanic lithic fragments (Figure 3). The matrix of the sandstone included mud and volcanic ash, with contents ranging from 5 to 20%. The cements of the sandstone were dominated by calcite, and the content of calcite was generally less than 8%, locally up to 13%. Based on the detection of XRD, there is a large amount of authigenic kaolinite and altered kaolinite, with an average content of 4%, even up to 15%. There is a medium to good sorting degree and lineal contact between grains in these sandstones.

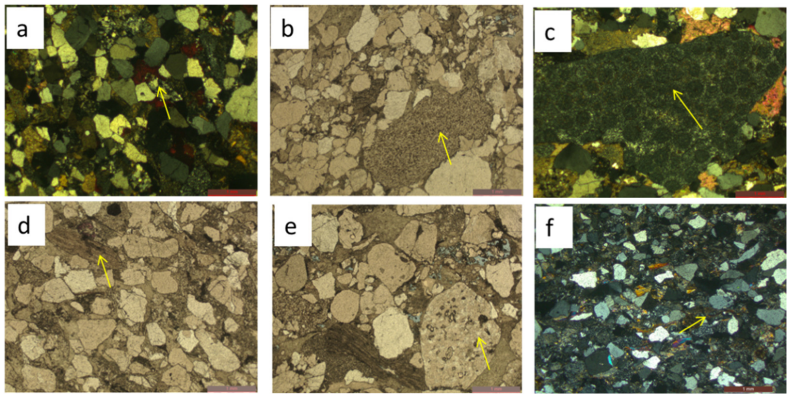

Figure 3. The types of lithic fragments in sandstones from the Shanxi Formation. (**a**) Metaquartzite fragment in medium sandstone, well D94, 2660.33 m, S2-1 sub-members. (**b**) Siltstone fragment in coarse-medium sandstone, well D41, 2600.76 m, S1-2 sub-members. (**c**) Oolitic limestone fragment in gravel-bearing coarse sandstone, well D94, 2660.33 m, S2-1 sub-members. (**d**) Mudstone fragment in mud-bearing medium sandstone, well D44, 2597.27 m, S1-2 sub-members. (**e**) Siliceous rock fragment in mud-bearing medium sandstone, well D41, 2621.82 m, S1-1 sub-members. (**f**) Phyllite rock fragment in medium sandstone, well D11, 2738.52 m, S2-1 sub-members. The yellow arrow shows the indicated minerals.

The grain size of the sandstone from the Shanxi Formation in the distributary channel is generally coarse. The coarse or medium-grained sandstones account for more than 90% of the total sandstone thickness. According to the grain size analysis, the median Φ of the sandstones of the Shanxi Formation ranges from −1.08 to 3.98 with an average of 0.64, which is coarse-grained. The standard deviation is 0.28 to 1.05, which is well to moderately sorted. The skewness is generally greater than 0, which has an obvious positive skewness. The sandstone texture is generally characterized by grain-supported, and the local mud-

bearing medium-grained sandstone has a heterogeneous matrix-supported texture. The detrital particles of the grain-supported sandstone are generally in line contact with each other, and only some samples are in point contact, indicating strong compaction. The mud-bearing medium sandstones were frequently observed in the cores (Figure 3d).

4.2. Diagenetic Alteration

There are mainly three types of diagenetic alteration in the sandstones from the Shanxi Formation. The dissolution of lithic fragments and feldspar is common in the sandstones (Figure 4a,b). As the by-product of lithic fragment dissolution, siliceous and kaolinite often remain in the dissolved pores (Figure 4a,b). The dissolution of feldspar occurs along the lattice twin crystal plane. As special minerals after dissolution of feldspar, the worm-like kaolinite could be observed (Figure 4e). There are different degrees of compaction in these sandstones (Figure 4c). The plastic lithic fragment, mica, mud, and volcanic ash are easy to compact under the overburdened load. The degree of compaction is closely related to the grain size and matrix content in the sandstones. The weakest compaction was in the coarse or coarse to medium sandstone, while the compaction of mud-bearing medium sandstone was strongest. The cementation could be observed in some sandstone, mainly cemented by calcite (Figure 4d), with minor silica. The highest content of calcite in sandstone was up to 13%. In addition, the kaolinite filling, quartz overgrowth, authigenic quartz, illitization, and chlorite coating (Figure 4f) were observed. The authigenic rutile and barite occurred in S1-2 and S1-3 submembers, identified by energy disperse spectroscopy. The smectite and illite ratio reflected thermal evolution in sandstone. The ratio of smectite/(smectite + illite) in sandstones from the Shanxi Formation ranges from 5–10%, showing that the middle diagenetic stage occurred in these sandstones. The main diagenetic alterations were dissolution, cementation, and compaction.

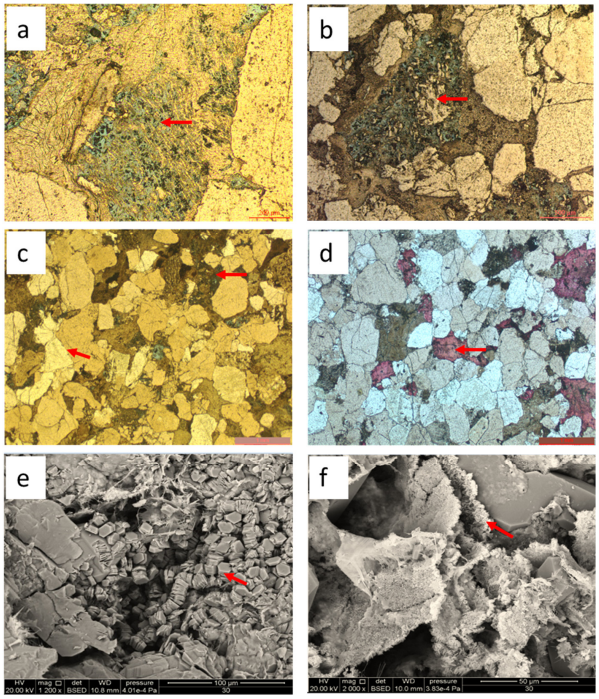

Figure 4. The diagenetic alteration in the sandstones from the Shanxi Formation (from the identification of thin sections). (**a**) The dissolution of a lithic fragment, well D69, 2705.01 m, S1-3 sub-members. (**b**) The dissolution of K-feldspar, well D41, 2600.76 m, S1-2 sub-members. (**c**) The compaction in the mud-bearing medium sandstone, well D44, 2551.12 m, S2-2 sub-members. (**d**) The calcite cementation and quartz overgrowth in sandstones, well D39, 2728.98 m, S2-2 sub-members. (**e**) The worm-like kaolinite filled in the dissolved pores, well D41, 2566.62 m, S2-1 sub-members. (**f**) The chlorite coating on the detrital grains in fine sandstone, well D41, 2566.62 m, S2-1 sub-members.

4.3. Single Sandbody Stacking Pattern

The lithofacies can reflect the hydrodynamic conditions over a period, and the single sandbody stacking pattern can reflect the change in the hydrodynamic conditions during the river deposition period. The sandbody stacking pattern could be the same in the same sedimentary microfacies, while the sandbody stacking pattern could contain two or more sedimentary microfacies. In this study, according to the variation of rock size in the vertical direction, the sandstone stacking patterns were divided into three patterns, mixed stacking patterns of coarse- to medium-grained sandstone (MSP), fining-upwards stacking patterns of coarse- to medium-grained sandstone (FSP), and coarsening-upwards stacking patterns of fine- to coarse-grained sandstone (CSP) (Figure 5). MSP bears sandstones with different grain sizes vertically. In the typical section of MSP, coarse-medium sandstone and interbedded coal seams developed in the upper and lower parts, and mud-bearing medium sandstone in the middle part. The occurrence of mud-bearing medium sandstone with a high content of matrix shows the characteristics of density flow. The MSP indicates intermittent strong but unstable hydrodynamic conditions. FSP has the fining-upward sequence. In the vertical section of FSP, medium-coarse sandstone develops in the lower part, the medium sandstone develops in the middle part, and the fine sandstone to siltstone develops in the upper part. The FSP represents the typical characteristics of the channel. CSP has the coarsening-upwards sequence. In the vertical section of CSP, coarse-medium sandstone develops in the upper part, and fine sandstone to siltstone occurs in the lower part develops. CSP frequently occurs in the mouth bar.

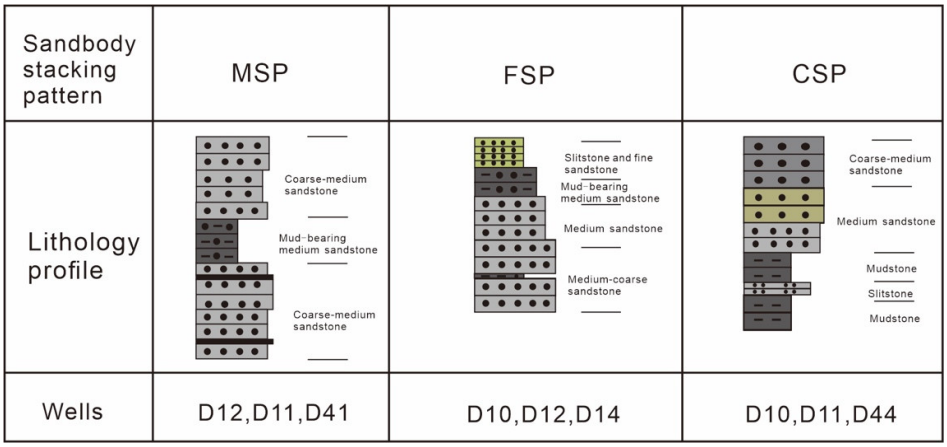

Figure 5. The single sandbody stacking pattern of Shanxi Formation in the study area.

According to the analysis of lithological profiles from 10 wells in the study area, the single sandbody stacking patterns of the Shanxi Formation are mainly dominated by FSP and MSP, and FSP is the most common. From statistics of the core, there are obvious lithofacies differences in the three stacking patterns (Figure 6). The lithofacies of MSP and FSP are mainly coarse or coarse to medium-grained sandstone overall, and predominantly massive texture. The lithofacies of CSP are mainly medium-grained sandstone and siltstone, which is a pattern with relatively fine particles.

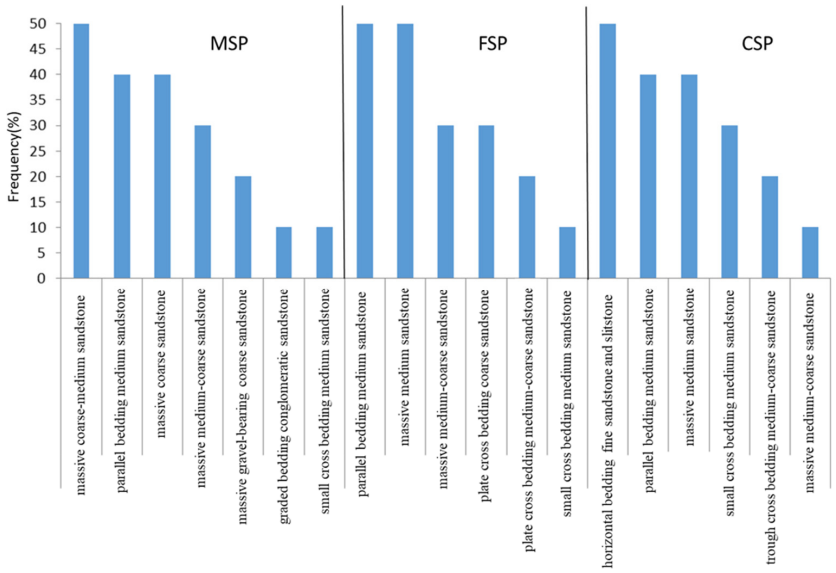

Figure 6. The occurrence frequency of lithofacies types in the different sandbody stacking patterns of the Shanxi Formation.

5. Discussion

5.1. The Relatively High-Porosity Lithofacies in Three Sandbody Stacking Patterns

The porosities and permeabilities of 59 samples show that the physical properties of the gravel-bearing coarse sandstone, coarse sandstone, and medium-coarse sandstone of the Shanxi Formation are relatively good, with average porosity generally greater than 4% and permeability greater than 0.5×10^{-3} μm^2. The physical properties of the mud-bearing medium sandstone and medium sandstone are poor, with the permeability of lower than 0.5×10^{-3} μm^2. There are obvious differences in porosity and permeability of the main lithofacies of the Shanxi Formation. Based on the comparison of the average porosity and average permeability of different lithofacies, the graded bedding conglomeratic sandstone, massive gravel-bearing coarse sandstone, plate cross-bedding coarse sandstone, and massive coarse sandstone are sandstones with high-quality reservoirs, with an average porosity greater than 8% and an average permeability greater than 1×10^{-3} μm^2 (Figure 7). According to the statistics of the development degree of these four types of relatively high porosity and permeability lithofacies in different single sandbody stacking patterns, the relatively high porosity and permeability lithofacies are mostly developed in MSP and FSP, especially in FSP (Figure 8). It can be seen that the single sandbody stacking patterns could influence the physical property of the sandstone reservoir.

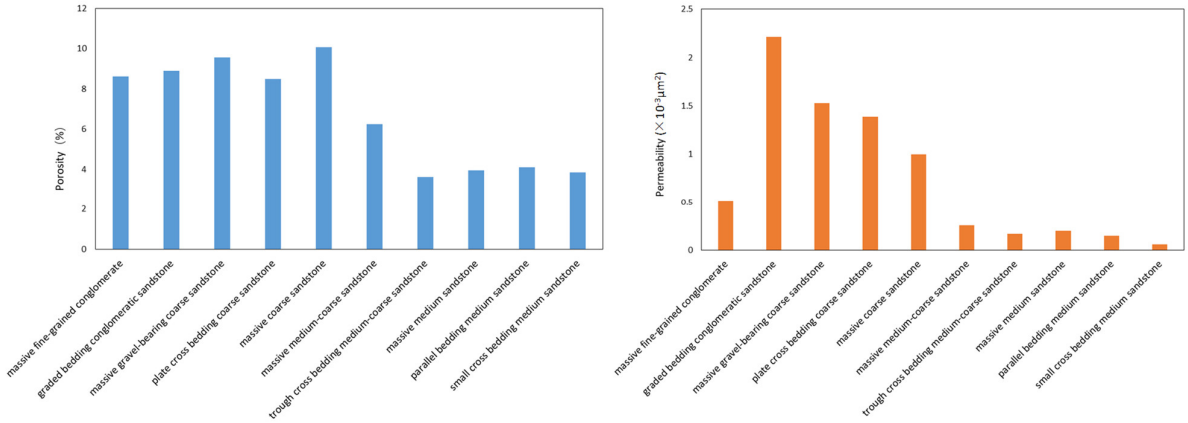

Figure 7. The average porosity and permeability of different lithofacies from the Shanxi Formation.

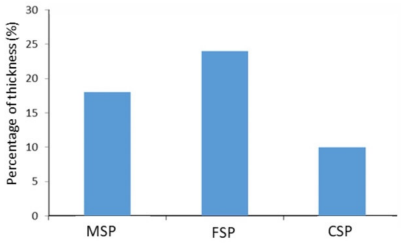

Figure 8. Percentage of thickness of relatively high porosity and permeability facies types in different sandbody stacking patterns.

5.2. The Difference of Components in Sandstones in Three Sandbody Stacking Patterns

The sedimentary hydrodynamic conditions during the formation of certain sandbody stacking patterns can lead to differences in components of sandstones, which have obvious effects on the reservoir's physical properties. The whole-rock analysis by XRD shows that the clastic particles of the sandstones from the Shanxi Formation in the study area are all dominated by quartz, followed by lithic fragments, and almost no feldspar could be detected (Table 2). The lithic fragment fractions include sedimentary rock, metamorphic rocks, volcanic rocks, mica, and a small amount of chert. The sedimentary rocks are dominant in all lithic fragment fractions. The statistical analysis of the components identified in thin sections shows that the relative percentages of quartz in MSP and FSP are higher than that in CSP, but the relative percentages of lithic fragments in MSP and FSP are lower than that in CSP. In other words, there is a relatively low content of quartz and relatively high lithic fragment content in CSP, especially the sedimentary lithic fragment (Figure 9). The compaction resistance of different lithic fragments varies greatly. Among all sedimentary lithic fragments, carbonate rocks have the strongest compaction resistance, followed by siltstones. Mudstones are easily compacted [31].

Table 2. The composition of sandstone rocks detected by XRD whole rock analysis.

No.	Mineral Species and Content (%)					Total Clay Minerals (%)
	Quartz	Potassium Feldspar	Plagioclase	Calcite	Dolomite	
1	85.1	0	0	0	0	14.9
2	81.3	0	0	0	0.8	17.9
3	93.3	0	0	0	0	6.7
4	84	0	0	0	1.5	14.5
5	85.3	0	0	0	3.7	11
6	78.3	0	0	0	2.3	19.4
7	76.8	0	0	0	4.5	18.7
8	87	0	0	0	2.1	10.9
9	81.9	0	0	0	0	18.1
10	77.7	0	0	0	2.2	20.1
11	80.9	0	0	1.3	0	17.8
12	77.7	0	0	2.5	0	19.8
13	83.8	0	0	0	0	16.2
14	94.3	0	0	0	0	5.7
15	94.5	0	0	0	0	5.5
16	93.7	0	0	0	0	6.3
17	88.8	0	0	0	0	11.2
18	92.7	0	0	0	0	7.3
19	85.1	0	0	0	0	14.9

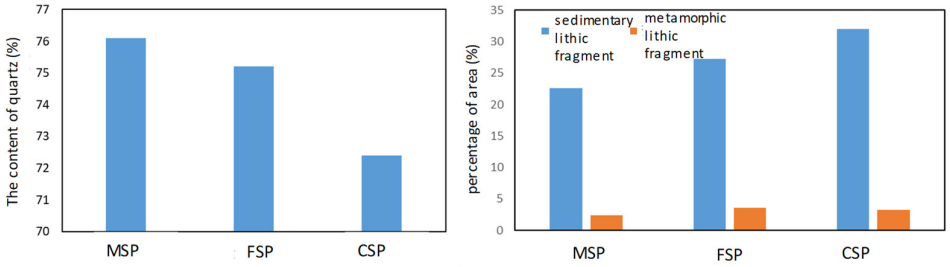

Figure 9. The difference of components in sandstones from different single sandbody stacking patterns.

The analysis of the relationship between the content of the matrix and the physical properties showed that there was an obvious negative correlation between the content of the matrix and both porosity and permeability in the sandstones with the grain-supported texture (Figure 10). Through statistical comparison of the content of matrix in the sandstones developed in different single sandbody stacking patterns, it was found that the content of matrix in CSP was significantly higher than that in MSP and FSP. The relatively high matrix in sandstones developed in CSP mainly resulted in the relatively poor physical properties.

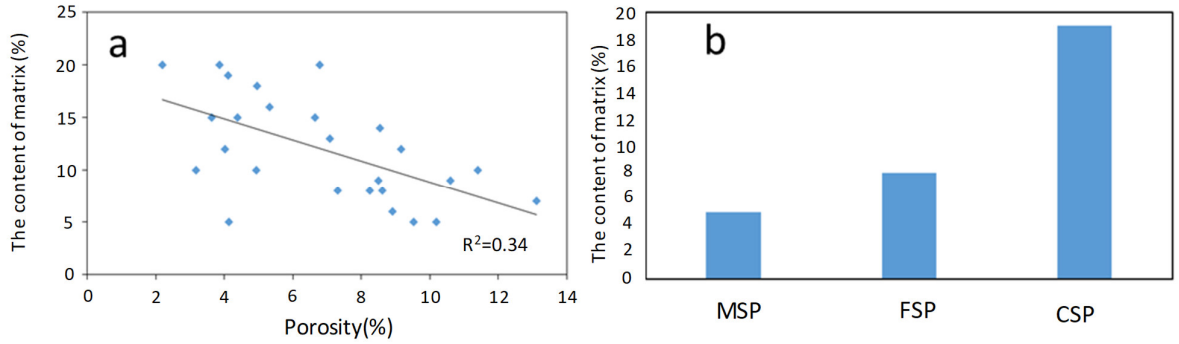

Figure 10. The matrix content of sandstones from different single sandbody stacking patterns. (**a**) Correlation between matrix content and porosity. (**b**) Comparison diagram of average matrix content of sandstone.

5.3. Differences in the Degree of Diagenesis in Three Sandbody Stacking Patterns

According to the analysis of the types of diagenesis in the Shanxi Formation, compaction and dissolution have an obvious influence on the physical properties of reservoirs. The strength of compaction is related to the particle size, content of plastic particles, burial depth, grain sorting, and degree of early cementation [9,32,33]. Sandstones with relatively weak compaction are able to retain more well-connected primary pores and have relatively high permeability. Under weak cementation, the primary pores in sandstones could be preserved well. By counting the degree of primary pore development in the sandstones in three sandbody stacking patterns, the proportions of primary pores in the sandstones from MSP and FSP are significantly higher than that in CSP (Figure 11), indicating that the sandstones in MSP and FSP experienced a lower degree of diagenesis than that in CSP, resulting from the high content of quartz and relatively lower content of sedimentary lithic fragments.

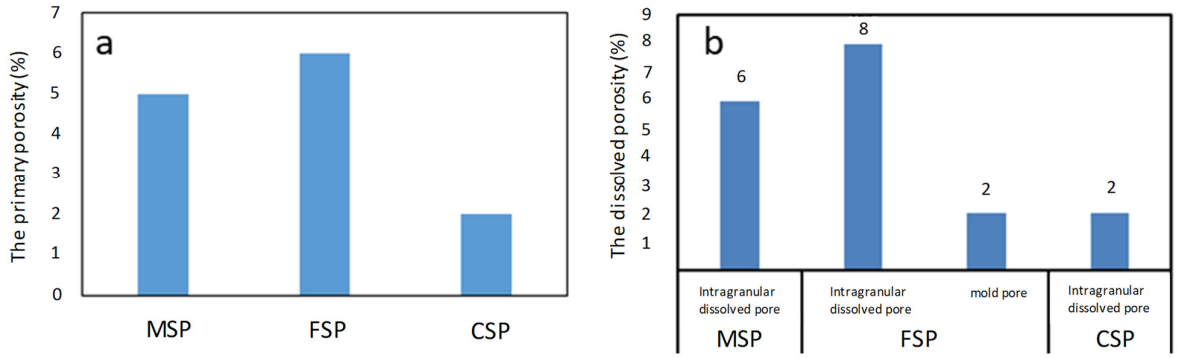

Figure 11. Comparative diagram of primary porosity and dissolved porosity in sandstone of different sandbody stacking patterns. (**a**) The primary porosity in sandstones of different sandstone stacking patterns. (**b**) The dissolved porosity in sandstones of different sandstone stacking patterns.

Dissolution is commonly developed in sandstones of the Shanxi Formation with grain-supported texture, but the degree of dissolution varies widely. There are some mold pores within detrital grains formed by intense dissolution locally. Through the observation of casting thin sections of sandstone and scanning electron microscopy observations, most dissolved pores in the sandstone from the Shanxi Formation were formed after lithic fragment dissolution, and some were formed by feldspar dissolution. As the product of feldspar dissolution, worm-like authigenic kaolinites can be observed (Figure 12). The degree of dissolution could be influenced by compaction [24]. Organic acids are easily circulated in the late diagenesis stages of sandstones with relatively weak compaction, contributing to the development of dissolution [17]. The amount of secondary dissolved pore space varies significantly among sandstones with different sandbody stacking patterns. As shown in Figure 12b, the dissolution pores are more developed in the sandstones from MSP and FSP, and some mold pores are developed in the sandstone from FSP. This different dissolution is produced by the original material composition of sandstones in the sandbody stacking patterns. The higher quartz content and lower sedimentary lithic fragment content of sandstones in MSP and FSP result in the ability to retain a certain number of primary pores during compaction, which leads to a stronger dissolution.

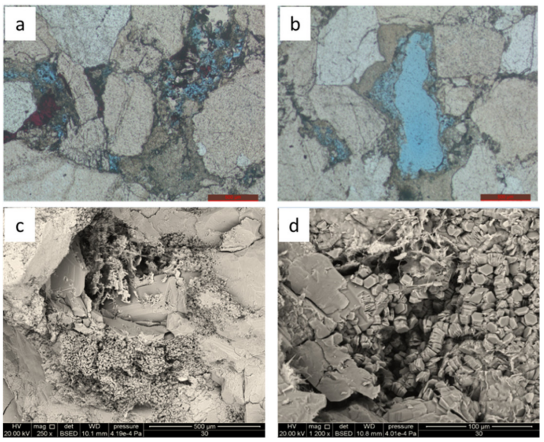

Figure 12. Characteristics of dissolved pores in sandstones of the Shanxi Formation. (**a**) Intragranular dissolved pores and residual intergranular pores. Thin section image, well D69, 2705.01 m, S1-3 sub-members. (**b**) Mold pore, thin section image, well D69, 2702.7 m, S1-3 sub-members. (**c**) The dissolution pore of the lithic fragment, SEM image, well D41, 2566.62 m, S2-1 sub-members. (**d**) Feldspar dissolution pores are filled with authigenic kaolinite, SEM image, well D41, 2566.62 m, S2-1 sub-members. The blue cast part indicates the pores in (**a**,**b**).

6. Conclusions

(1) The lithofacies with relatively high porosity and permeability in the Shanxi Formation are the graded bedding conglomeratic sandstone, massive gravel-bearing coarse sandstone, plate cross-bedding coarse sandstone, and massive coarse sandstone. The average porosity of the four lithofacies is greater than 8%, and their average permeability is greater than 1×10^{-3} μm^2.

(2) According to the change of sedimentary structure and lithology vertically, the single sandbody stacking pattern can be divided into three types, including mixed stacking patterns of coarse- to medium-grained sandstone (MSP), fining-upwards stacking patterns of coarse- to medium-grained sandstone (FSP), and coarsening-upwards stacking patterns of fine- to coarse-grained sandstone (CSP). MSP and FSP are two types of single sandbody stacking patterns with relatively good physical properties.

(3) The original components lead to the different physical properties of sandstones from different single sandbody stacking patterns. There is a relatively high content of quartz, low content of sedimentary lithic fragments, and low content of matrix in sandstones from the MSP and FSP compared to the CSP, resulting in the preservation of primary pores during compaction and the formation of dissolved pores. This study has illustrated that the physical property differences of sandstones in different single sandbody stacking patterns are not clear and can improve the accuracy of high-quality sandstone reservoir predictions.

Author Contributions: Writing—original draft preparation, and writing—review and editing, Y.H.; methodology, resources, and supervision, H.G.; validation, formal analysis, investigation, H.L.; data curation, visualization, software, C.L.; conceptualization, M.F. All authors have read and agreed to the published version of the manuscript.

Funding: This research was funded by Study on controlling factors of Shanxi Formation reservoir development in Da28 well area, grant number 80303-AHE081.

Institutional Review Board Statement: Not applicable.

Informed Consent Statement: Not applicable.

Data Availability Statement: Not applicable.

Acknowledgments: We thank Yan Shuhong, Li Xiaohui, Ren Guanglei for their contribution to sampling.

Conflicts of Interest: The authors declare no conflict of interest.

References

1. Leila, M.; El Sharawy, M.; Bakr, A.; Mohamed, A.K. Controls of facies distribution on reservoir quality in the Messinian incised-valley fill Abu Madi Formation in Salma delta gas field, northeastern onshore Nile Delta, Egypt. *J. Nat. Gas Sci. Eng.* **2022**, *97*, 104360. [CrossRef]
2. Gould, K.M.; Piper DJ, W.; Pe-Piper, G. Lateral variation in sandstone lithofacies from conventional core, Scotian Basin: Implications for reservoir quality and connectivity. *Can. J. Earth Sci.* **2012**, *49*, 1478–1503. [CrossRef]
3. Stroker, T.M.; Harris, N.B.; Elliott, W.C.; Wampler, J.M. Diagenesis of a tight gas sand reservoir: Upper Cretaceous Mesaverde Group, Piceance Basin, Colorado. *Mar. Pet. Geol.* **2013**, *40*, 48–68. [CrossRef]
4. Burki, M.; Darwish, M. Electrofacies vs. lithofacies sandstone reservoir characterization companion sequence, Arshad gas/oil field, Central Sirt Basin, Libya. *J. Afr. Earth Sci.* **2017**, *130*, 319–336. [CrossRef]
5. Taylor, T.R.; Giles, M.R.; Hathon, L.A.; Diggs, T.N.; Braunsdorf, N.R.; Birbiglia, G.V.; Kittridge, M.G.; Macaulay, C.I.; Espejo, I.S. Sandstone diagenesis and reservoir quality prediction: Models, myths, and reality. *AAPG Bull.* **2010**, *94*, 1093–1132. [CrossRef]
6. Du, W. Study on the Stratigraphic Sequence Stratigraphy, Sedimentary Phase and Reservoir of Shanxi Formation in Daniudi Gas Field, Ordos Basin. Ph.D. Thesis, China University of Geosciences, Beijing, China, 2013.
7. Kathleen, G.; Georgia, P.; David, J.W.P. Relationship of diagenetic chlorite rims to depositional facies in Lower Cretaceous reservoir sandstones of the Scotian basin. *Sedimentology* **2010**, *57*, 587–610.
8. Straub, K.M.; Mohrig, D.; Buttles, J.; McElroy, B.; Pirmez, C. Quantifying the influence of channel sinuosity on the depositional mechanics of channelized turbidity currents: A laboratory study. *Mar. Pet. Geol.* **2011**, *28*, 744–760. [CrossRef]

9. Saïag, J.; Brigaud, B.; Portier, É.; Desaubliaux, G.; Bucherie, A.; Miska, S.; Pagel, M. Sedimentological control on the diagenesis and reservoir quality of tidal sandstones of the Upper Cape Hay Formation (Permian, Bonaparte Basin, Australia). *Mar. Pet. Geol.* **2016**, *77*, 597–624. [CrossRef]
10. Zhang, Y. Research on the Prediction Technology of High-Quality Reservoirs in Low-Porosity Sandstone in Tabamiao Area of Ordos Basin. Ph.D. Thesis, China University of Geosciences, Beijing, China, 2008.
11. Yin, S.; Chen, G.; Zhang, L.; Luo, Y.; Wang, C. The control of petrographic configuration on dense sandstone quality reservoirs: An example from the Shu II section of the Sichuan West Depression. *Nat. Gas Geosci.* **2016**, *27*, 1179–1189.
12. Lin, J.; Zhang, X.; Lin, C.; Duan, D.; Huang, X.; Sun, X.; Dong, C. Reservoir evolution characteristics of deep dense sandstone gas reservoirs under petrographic constraints. *Pet. Nat. Gas Geol.* **2019**, *40*, 886–899.
13. Song, J.G.; Gao, W.L. Introduction to the Chinese Petroleum Geology Journal. *J. Pet.* **1991**, *2*, 141.
14. Zhang, X.; Fu, M.; Deng, H.; Li, Z.; Zhao, S.; Gluyas, J.G.; Ye, T. The differential diagenesis controls on the physical properties of lithofacies in sandstone reservoirs from the Jurassic Shaximiao Formation, westernSichuan depression, China. *J. Pet. Sci. Eng.* **2020**, *193*, 107413. [CrossRef]
15. Zhang, R. Evaluation and Capacity Prediction of Low-Porosity Reservoirs in Da Niu Di Area. Master's Thesis, Chengdu University of Technology, Chengdu, China, 2016.
16. Wei, X.P.; Hu, X.; Li, H.; Zhao, J.; Zhao, L.S. Evaluation of horizontal well logging in tight sandstone gas reservoirs—Example of well area X in Daniudi gas field in Ordos Basin. *Pet. Nat. Gas Geol.* **2019**, *40*, 1084–1094.
17. Qin, W. Study on Fluid Characteristics and Gas Transport Pattern in the Upper Paleozoic of Daniudi Gas Field. Master's Thesis, Chengdu University of Technology, Chengdu, China, 2011.
18. Wang, Z.; Chen, H.; Zhang, J. Evolution of Late Paleozoic sedimentary system and coal-formed gas reservoirs in Ordos Basin. *Sediment. Tethys Geol.* **2002**, *2*, 18–23.
19. Wang, G. Research on the Genesis and Evaluation of Dense Sandstone Reservoir in Daniudi Gas Field. Master's Thesis, China University of Petroleum, Beijing, China, 2010.
20. Chen, H.; Li, J.; Zhang, C.; Cheng, L.; Cheng, L. Discussion on the depositional environment of the Shanxi Formation in the Ordos Basin and its geological insights. *J. Petrol.* **2011**, *27*, 2213–2229.
21. Zhang, G.; Chen, S.; Guo, S. Sedimentary phases of the Shanxi Formation in the Daniudi Gas Field, northeastern Ordos Region. *Pet. Nat. Gas Geol.* **2011**, *32*, 388–396+403.
22. Yuan, F. Depositional environment and reservoir characteristics of high-yielding gas reservoirs in Box 3 section of Daniudi gas field. *Pet. Geol. Eng.* **2008**, *22*, 18–20.
23. Zhang, J. Study on Logging Interpretation Model of Tight Sandstone Gas Reservoir in Da 66 Well Area. Master's Thesis, China University of Petroleum (East China), Dongying, China, 2015.
24. Wang, S. Study on the Spreading of Sand Bodies of Taiyuan Formation in Tabamiao Area. Master's Thesis, Chengdu University of Technology, Chengdu, China, 2006.
25. Zheng, T. Evaluation of Tight Sandstone Gas Formation in Shan2 Section of Daniudi Gas Field. Master's Thesis, Chengdu University of Technology, Chengdu, China, 2015.
26. Luo, D.; Tan, X.; You, Y.; Liu, J.; Feng, Q.; Liu, Z. A comparative approach to stratigraphic delineation in areas with complex sedimentary environments: An example from the Daniudi gas field in the Ordos Basin. *Pet. Nat. Gas Geol.* **2008**, *1*, 38–44.
27. Wan, Y.; Li, Z.; Peng, C.; Kong, W.; Xie, Y.; Zheng, T. Characteristics and evaluation of dense sandstone reservoirs in the Shan II section of the Daniudi gas field in the Ordos Basin. *Miner. Rocks* **2016**, *36*, 106–114.
28. Harms, J.C.; Fahnestoek, R.K. Stratification, bedforms, and flow phenomena (with an example from the Rio Grande). *SEPM Spec. Publ.* **1977**, *12*, 84–115.
29. Liu, Z.; Hu, Y. Pore structure characteristics of the Shan1 section of the Shanxi Group reservoir in the Daniudi gas field. *Broken Block Oil Gas Field* **2008**, *5*, 37–39.
30. Li, C.; Qiu, Q.; Liang, Y.; Li, Z.; Li, H. Study of sedimentary microphases in Shan 1 section of the Daniudi gas field in the Ordos Basin. *Henan Sci. Technol.* **2015**, *4*, 103–104.
31. Mansurbeg, H.; De Ros, L.F.; SMorad, J.M.; Ketzer, M.A.K.; El-Ghali, M.A.; Caja, R. Othman. Meteoric-water diagenesis in late Cretaceous canyon-fill turbidite reservoirs from the Espírito Santo Basin, eastern Brazil. *Mar. Pet. Geol.* **2012**, *37*, 7–26. [CrossRef]
32. Wang, W.; Lin, C.; Zhang, X.; Dong, C.; Ren, L.; Lin, J. Structural controls on sandstone compaction within the anticline crest and flank: An example from the Xihu Sag, East China Sea Basin. *J. Pet. Sci. Eng.* **2022**, *211*, 110157. [CrossRef]
33. Yan, Y.; Zhang, L.; Luo, X.; Liu, K.; Yang, B.; Jia, T. Simulation of ductile grain deformation and the porosity loss predicted model of sandstone during compaction based on grain packing texture. *J. Pet. Sci. Eng.* **2022**, *208*, 109583. [CrossRef]